

## Towards ferromagnetic quantum criticality in $\text{FeGa}_{3-x}\text{Ge}_x$ : $^{71}\text{Ga}$ NQR as a zero-field microscopic probe

M. Majumder,<sup>1,\*</sup> M. Wagner-Reetz,<sup>1</sup> R. Cardoso-Gil,<sup>1</sup> P. Gille,<sup>2</sup> F. Steglich,<sup>1</sup> Y. Grin,<sup>1</sup> and M. Baenitz<sup>1</sup>

<sup>1</sup>Max Plank Institute for Chemical Physics of Solids, 01187 Dresden, Germany

<sup>2</sup>Ludwig-Maximilians-Universität München, 80539 Munich, Germany

(Received 7 October 2015; revised manuscript received 18 January 2016; published 5 February 2016)

$^{71}\text{Ga}$  NQR, magnetization, and specific-heat measurements have been performed on polycrystalline Ge-doped  $\text{FeGa}_3$  samples. A crossover from an insulator to a correlated local moment metal in the low-doping regime and the evolution of itinerant ferromagnet upon further doping is found. For the nearly critical concentration at the threshold of ferromagnetic order,  $x_c = 0.15$ ,  $^{71}(1/T_1T)$  exhibits a pronounced  $T^{-4/3}$  power law over two orders of magnitude in temperature, which indicates three-dimensional quantum critical ferromagnetic fluctuations. Furthermore, for the ordered  $x = 0.2$  sample ( $T_c \approx 6$  K),  $^{71}(1/T_1T)$  could be fitted well in the frame of Moriya's self-consistent renormalization theory for weakly ferromagnetic systems with  $1/T_1T \sim \chi$ . In contrast to this, the low-doping regime nicely displays local moment behavior where  $1/T_1T \sim \chi^2$  is valid. For  $T \rightarrow 0$ , the Sommerfeld ratio  $\gamma = (C/T)$  is enhanced (70 mJ/mole  $\text{K}^2$  for  $x = 0.1$ ), which indicates the formation of heavy  $3d$  electrons.

DOI: [10.1103/PhysRevB.93.064410](https://doi.org/10.1103/PhysRevB.93.064410)

### I. INTRODUCTION

Strongly correlated electron systems exhibit unconventional magnetic and electronic properties due to the presence of competing interactions. As a consequence of this competition combined with quantum fluctuations, the critical temperatures of phase transitions may continuously approach zero and a quantum critical point (QCP) emerges. QCPs are located therefore at zero temperature and they cause quantum fluctuations between competing ground states when a material is continuously tuned with a parameter (chemical pressure, mechanical pressure, magnetic field, etc.) [1,2]. Recently, spatial dimensionality of a material has been demonstrated as an insightful ingredient in tuning the degree of fluctuations and the physics of quantum criticality [3]. Quantum critical fluctuations cause non-Fermi-liquid (NFL) behavior and divergencies in physical properties, e.g., the effective charge carrier mass [4].

While, to date, several antiferromagnetic (AFM) quantum criticality (QC) systems have been studied extensively in  $4f$  and  $3d$  systems, the quest for ferromagnetic quantum criticality (FMQC) is of great interest [5]. This continues to be a less explored topic compared to AFMQCs, simply because FMQCPs are commonly avoided in two ways: It has been seen that pressure can decrease the FM transition temperature down to a reasonably low temperature, but just before reaching the FMQCP, the transition changes from second order to first order and the pure FMQCP is wiped out [6]. Isovalent or aliovalent substitutions can also systematically reduce the ordering temperature before some AFM order or a more complex phase develops. Usually the substitution creates strong disorder, which then forms a Kondo cluster glass state [7] or other, more glassy states, such as the Griffith phases [8,9]. Furthermore, spiral spin arrangements [10] or competing correlations (FM versus AFM) [11–14] have also

been found in some systems which prevents the formation of a pure FMQCP. It is therefore not surprising that a FMQCP has so far been verified only in one material, i.e., the  $4f$  Kondo lattice system  $\text{YbNi}_4(\text{P}_{0.9}\text{As}_{0.1})_2$  [15].

According to theoretical investigation in itinerant three-dimensional (3D) and 2D systems, the FMQCP is unstable [16–18] and actually the system approaches to an incommensurate ordering or a first order into a commensurate state [16–18], as experimentally observed. According to Chubukov *et al.*, a system may undergo a Pomeranchuk instability into a  $p$ -wave spin-nematic state before a FM QCP is reached [17].

For the  $3d$  intermetallic system, the search for new quantum critical matter has various approaches. The first one was to study itinerant  $3d$  magnets at the verge of ferromagnetic order ( $\text{NbFe}_2$  [19],  $\text{Ta}(\text{Fe},\text{V})_2$  [20]) and a second one was on diluted Fe-based systems ( $\text{YFe}_2\text{Al}_{10}$  [21],  $\text{YbFe}_2\text{Al}_{10}$  [22]). A third approach was to study nonmagnetic  $3d$ -based semimetals (Fe, Co, Cr). Among them, binary Fe-based semimetals such as  $\text{FeSi}$ ,  $\text{FeSb}_2$ , and  $\text{FeGa}_3$  earned great attention because of their strong correlations evolving at low temperatures accompanied by large thermopower peaks, which makes them promising candidates for thermoelectrics [23–25]. Here, metallic behavior and Fe-based magnetism can be introduced by various substitutions. In contrast to the Te substitution in  $\text{FeSb}_2$  (where Griffith phases evolve due to disorder) [9], Ge-doped  $\text{FeGa}_3$  has been claimed to be a system with much less disorder [26,27] where pure FMQC might be observed.  $\text{FeSb}_2$  and  $\text{FeGa}_3$  itself are already at the verge of correlations, as seen from NQR measurements where, at low temperature, fluctuation effects on  $1/T_1$  have been seen and have been successfully described by the “correlated” in-gap states model for both systems [28,29]. To explain the experimental phase diagram of electron- or hole-doped  $\text{FeGa}_3$ , theoretical calculations predicted that the systems turned into half metallic upon electron or hole substitution [30]. Small Co substitution in  $\text{FeGa}_3$  furnishes metallic behavior along with AFM correlations. Surprisingly, these correlations resemble

\*mayukh.cu@gmail.com

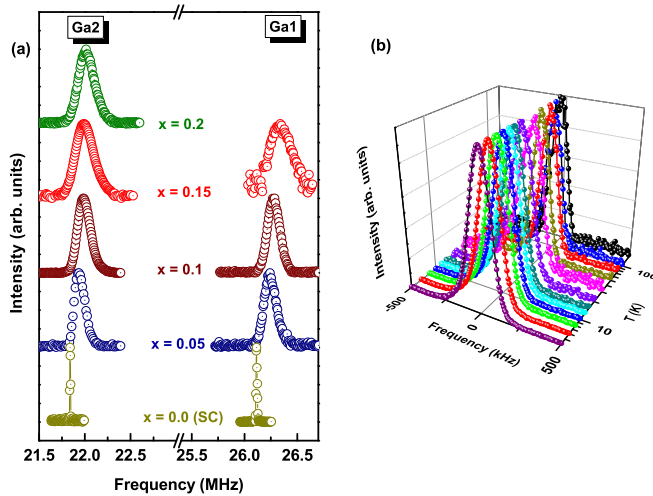


FIG. 1. (a)  $^{71}\text{Ga}$  NQR spectra for  $x = 0.0$  (single crystal), 0.05, 0.1, and 0.2 samples at 6 K. (b) Temperature dependence of NQR spectra of Ga2 site for the  $x = 0.1$  sample around the center frequency of  $\nu_0 = 22$  MHz.

heavy-fermion behavior, which indicates a localization of Fe moments [29]. Large Co substitution, however, creates large disorder, evidenced by broad Ga-NQR lines [31]. Nonetheless, it could be speculated that doped semiconductors opens up a new route for correlated  $d$ -electron physics.  $\text{Fe}(\text{Ga},\text{Ge})_3$  seems to be an ideal platform to study the evolution of a metallic magnetic state and furthermore to study the system exactly at the putative FMQCP.

Here we employ nuclear quadrupolar resonance (NQR) on the two Ga sites to explore the magnetic fluctuations in zero field on a microscopic scale over the entire phase diagram. There are mainly two important aspects of these studies. First NQR is a zero-field probe so the field effect on magnetic correlations [of Ruderman-Kittel-Kasuya-Yosida (RKKY) type, Kondo type] is absent. The second important aspect is related to the local character of the method. Usually in NQR the line position is given by the local electric field gradient (EFG) and the linewidth is governed by local disorder and local transferred fields (under the presence of magnetic ion). Therefore, information about local disorder and magnetic order is obtained simultaneously to the spin fluctuations.

## II. RESULTS AND DISCUSSIONS

Two  $^{71}\text{Ga}$  NQR lines are found for each sample, which corresponds to the two crystallographic Ga sites being present in the structure [Fig. 1(a)]. The NQR line positions of the parent compound are in good agreement with the previous obtained result on powder material [29]. The linewidth in Fig. 1(a) is much smaller than the reported results [29] due to the use of high-quality single crystals. The nearly isotropic and narrow linewidth indicates the absence of strong local disorder in this series, which is rather important to study FM critical phenomena. As the Ge concentration increases, the linewidth increases slightly. There is no considerable

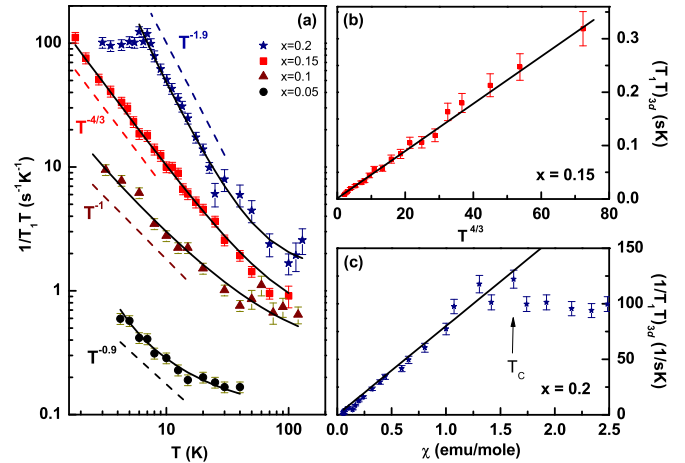


FIG. 2. (a) Temperature dependence of  $1/T_1T$  for the Ga2 site and the fitted dashed line corresponds to the power law at low temperatures and the solid line corresponds to Eq. (1). (b)  $(T_1T)_{3d}$  vs  $T^{4/3}$  for  $x = 0.15$ . (c)  $(1/T_1T)_{3d}$  vs  $\chi$  at  $\mu_0H = 0.005$  T for  $x = 0.2$ .

temperature dependence of the NQR frequency and linewidth for all samples. Figure 1(b) shows the temperature dependence for  $x = 0.1$  as an example. It should be mentioned that above the critical concentration  $x_C \approx 0.15$ , the width gets broadened (see Supplemental Material [32]).

The nuclear spin-lattice relaxation time ( $T_1$ ) has been measured for the  $^{71}\text{Ga}$  isotope for both of the Ga sites through the evolution of critical fluctuations at zero field throughout the phase diagram. The temperature dependence of  $1/T_1T$  has been plotted in Fig. 2(a) for the Ga2 site. To model the temperature dependence of  $1/T_1T$ , we applied a two-relaxation-channel model with

$$1/T_1T = R_{3d} + R_{CE} = (1/T_1T)_{3d} + (1/T_1T)_{CE}, \quad (1)$$

where the first term derives from transferred Fe 3d magnetic spin fluctuations and the second term is the uncorrelated conduction electron contribution. At high temperatures, the conduction electron term dominates, which gives a  $(1/T_1T)_{CE} = \text{const}$  term, known as the Korringa term. Here it could be speculated that upon doping with Ge at the Ga site, the density of states (DOS) at the Fermi level increases, which lead to an increase in  $(1/T_1T)_{CE}$  because  $(1/T_1T)_{CE} \sim N(E_F)^2 \sim (C/T)_{CE}^2$ . This is indeed the case for our samples (see Table 2 in the Supplemental Material [32]). Towards low temperatures, the term  $(1/T_1T)_{3d} \sim \sum_q A_q^2 \chi''(q, \omega)$  dominates. The isotropic approach to model the low-temperature upturn of  $1/T_1T$  is a simple power law,  $(1/T_1T)_{3d} \sim C/(T^n - \Theta) \sim AT^{-n}$  (if  $\Theta$  goes to zero), frequently used for other correlated systems at the proximity to the magnetic order.

$1/T_1T$  measured on both Ga sites for the same sample shows a similar temperature dependence, which indicates that both Ga sites are experiencing the same hyperfine field fluctuations [linearity of  $1/T_1T$  (Ga1) versus  $1/T_1T$  (Ga2) in Fig. 3] but with a dissimilar magnitude, which is due to the difference in hybridization of the Ga orbitals with Fe 3d orbitals. The slope of  $R_1$  vs  $R_2$  (Fig. 3) for each sample is

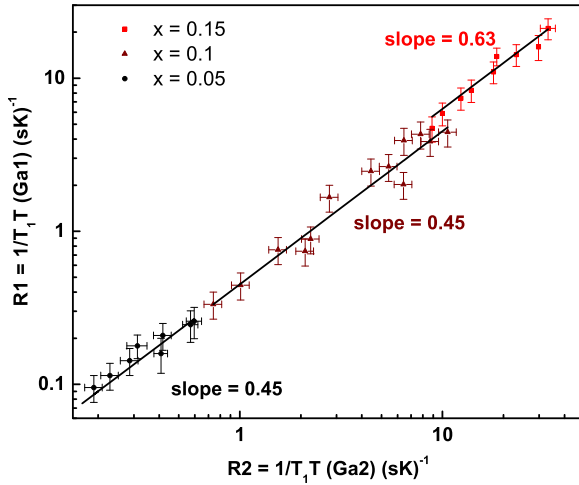


FIG. 3.  $R_1$  vs  $R_2$  for various samples with the temperature as an implicit parameter. Straight lines indicate a linear dependence for a particular sample.

always smaller than one and roughly independent of the doping level, which indicates that the Ga2 site is always experiencing a stronger hyperfine coupling than that of the Ga1 site. The Ga2 site has three Fe neighbors, whereas the Ga1 site has only two neighbors, which might lead to a smaller  $T_1$  value for the Ga2 site with respect to the Ga1 site. It seems from the crystal structure that the direction of the principle component of the electric field gradients ( $V_{zz}$ ) is different at different Ga sites, as  $1/T_1$  in NQR probes the spin fluctuations perpendicular to the direction of the principle component of the electric field gradients ( $V_{zz}$ ) tell us that in our case, electron spin fluctuations are rather isotropic.

For the critical sample with  $x = 0.15$ , the exponent equals  $n = 4/3$  over two decades of temperature, which is highly consistent with the existence of three-dimensional ferromagnetic quantum critical fluctuations [Fig. 2(a)] expected from the self-consistent renormalization (SCR) theory [33]. Furthermore, it can be easily seen from the  $(T_1T)_{3d}$  versus  $T^{4/3}$  plot in Fig. 2(b) that the dynamical spin susceptibility [ $\chi''(q, \omega)$ ] diverges almost at  $T = 0$ , which gives evidence that the critical fluctuations are quantum in nature for the  $x = 0.15$  system (whereas for the other samples it has a finite value shown in Fig. 5). The coefficient of electronic specific heat,  $C(T)/T$ , shows a logarithmic divergence (see Fig. S6(c) in the Supplemental Material [32]),  $\ln(T_0/T)$  (with  $T_0 \simeq 49$  K), which is expected near an itinerant 3D FMQCP. Below 1 K,  $C(T)/T$  seems to saturate, which might indicate that the  $x = 0.15$  sample does not exactly match the FMQCP but is located in the higher-doping side of the exact FMQCP. Furthermore, the field dependence of  $C/T$  follows a scaling relation in the  $C/T(0) - C/T(H)$  vs  $T/B^{0.6}$  plot (see Fig. S8 in the Supplemental Material) within the temperature range 1 to 5 K and field range 0.01 to 14 T, which indicates the quantum critical nature of spin fluctuations for  $x = 0.15$ .

The temperature dependence of  $1/T_1T$  in the paramagnetic region ( $T > T_C$ ) of the ordered sample ( $x = 0.2$ ) is linear to the bulk susceptibility  $\chi(T)$  [Fig. 2(c)] and also linear to

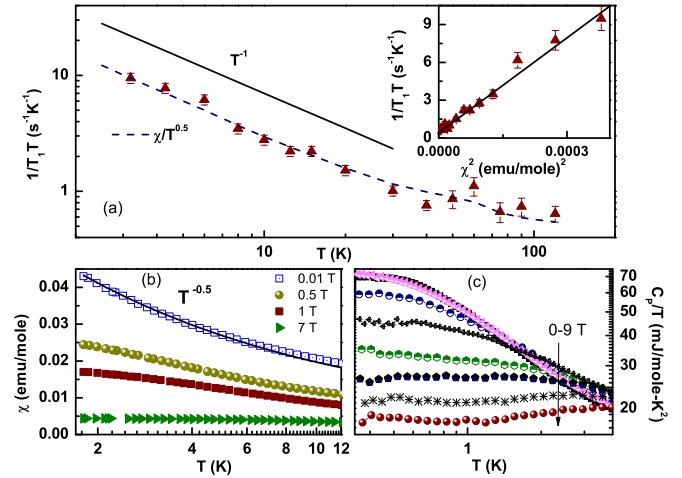


FIG. 4. (a) Temperature dependence of  $1/T_1T$  for  $x = 0.1$ . The solid line indicates the power law of  $T^{-1}$  and the dashed line is the fit according to Eq. (2); the inset shows  $1/T_1T$  vs  $(M/H)^2$  at  $\mu_0H = 0.01$  T with a solid line as a linear fit. (b),(c)  $T$  dependence of  $\chi = M/H$  and  $C(T)/T$  at different fields, respectively.

$C(T)/T$  [32], both showing a  $T^{-1.9}$  power law, which is a fingerprint of a weakly 3D itinerant ferromagnet predicted by SCR theory [34–36]. The absence of a clear peak in  $1/T_1T$  as well as in  $(C/T)$  [32] at the ordering temperature for  $x = 0.2$  indicates that the ordering might not be long-range order or in such higher doping range that there might be disorder. Below 6 K,  $C(T)/T$  deviates from power-law behavior and tends to saturate [32]. It has also been seen that below the ordering temperature, there is an onset of irreversible magnetic behavior seen in field-cooled–zero-field-cooled (FC-ZFC) magnetization measurements [32] for  $x = 0.2$ , indicative of a disordered state, and also the ZFC magnetization shows a peak at the ordering temperature, which indicates the presence of weak AFM correlations on the top of dominant FM correlations (see Supplemental Material [32]). Unusual states near ferromagnetic quantum criticality have been proposed by theory due to the competing interactions [37] and, in our case, it may be the competition between dominating FM and weak AFM correlations that induces such states near a FMQCP, although the effect of disorder or phase separation in this high-doping side cannot be fully discarded (see Supplemental Material [32]).

For small concentrations,  $1/T_1T$  increase with  $T^{-1}$  at low temperatures, which indicates the formation of a heavy electron out of the low density of carriers. This is confirmed by the increase of the Sommerfeld coefficient plotted as a function of temperature in Fig. 4(c). Similar to other heavy-fermion systems,  $1/T_1T$  could be modeled [38–42] for  $T > T_K$ ,

$$1/T_1T \propto \chi(T)/\Gamma, \quad (2)$$

with  $\Gamma \propto T^{0.5}$  and where  $\Gamma$  is the dynamic relaxation rate of the local moment [Fig. 4(a)]. Furthermore,  $1/T_1T \propto (\chi)^2$  was found [inset of Fig. 4(a)], which indicates that the Korringa law is valid and  $\chi \sim 1/\sqrt{T}$ , which is indeed the case [Fig. 4(b)]. Furthermore, the  $(C/T)$  value at the lowest temperature is about 70 mJ/mole  $K^2$ , which signals heavy-fermion behavior.

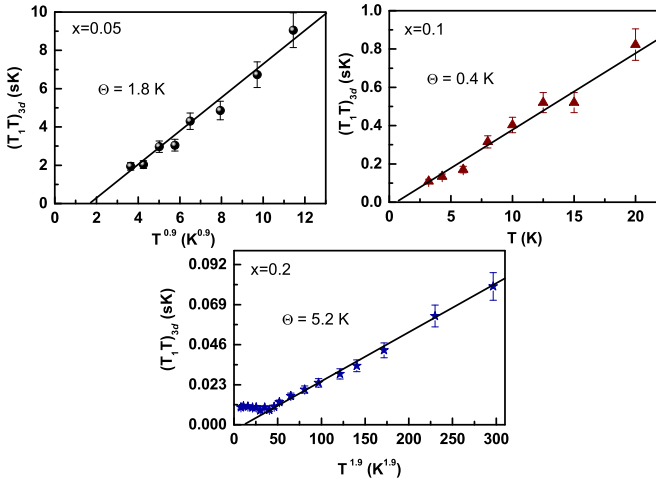


FIG. 5.  $(T_1 T_1)_{3d}$  vs  $T^n$  for various samples. The solid lines indicate a fit to  $1/T_1 T_1 \sim A/(T^n - \Theta)$  with given  $\Theta$  values.

The divergence of  $\chi(T)$  and  $C(T)/T$  at low fields can be suppressed by applying an external magnetic field [Figs. 4(b) and 4(c)] [32].

Additional evidence for the change of correlations with Ge substitution has been provided by the Wilson ratio  $R_W = \frac{\pi^2 R}{3C} \frac{\chi(0)}{\gamma}$ , where  $R$  is the ideal gas constant,  $C$  is the Curie constant,  $\chi(0)$  is the low-temperature susceptibility, and  $\gamma$  is the electronic specific-heat coefficient. The  $R_W$  values at 2 K for  $x = 0.05, 0.1, 0.15,$  and  $0.2$  are 3.9, 1.8, 130, and 215, respectively. For the low-doping systems ( $x = 0.05$  and  $0.1$ ), a value of  $R_W$  around 2 is compatible with a heavy-fermion system and, for the nearly critical ( $x = 0.15$ ) and the ordered system ( $x = 0.2$ ), the highly enhanced  $R_W$  value indicates strong ferromagnetic correlations.

As a summary, the full phase diagram of Ge-doped  $\text{FeGa}_3$  systems is plotted in Fig. 6. The low substituted Ge ( $x \leq 0.15$ ) systems exhibit a heavy-fermion behavior. Increasing Ge concentration ( $x \geq 0.15$ ) promotes the evolution of ferromagnetic correlations, and three-dimensional quantum critical fluctuation have been confirmed for the  $x = 0.15$  sample.  $1/T_1 T$  at the lowest temperature (2 K) as a function of  $x$  (depicted by  $R_{3d}$  in the upper panel of Fig. 6) indicates a divergence of dynamical spin susceptibility at the critical concentration, commonly found in those systems in the vicinity to the QCP. One can also estimate the critical temperature [ $\Theta$  (K)], where the dynamical spin susceptibility diverges [see Figs. 2(c) and 5];  $\Theta$  (K)  $\simeq 0$  for  $x = 0.15$ , but for the other systems, it has a finite value (Fig. 5), which indicates that the  $x = 0.15$  sample resides close to the FMQCP (Fig. 6). Larger substitutions of Ge ( $x \geq 0.2$ ) convert the short-range ordering to long-range ferromagnetic ordering. Upon increasing Ge content,  $1/T_1 T$  evidences an enhancement of both DOS and the correlations between Fe moments, which induce long-range FM order (evident from the increment of  $n$  in the lower panel of Fig. 6).

### III. CONCLUSION

In conclusion  $^{71}\text{Ga}$  NQR, magnetization, and specific-heat measurements have been performed in a  $\text{FeGa}_{3-x}\text{Ge}_x$  poly-

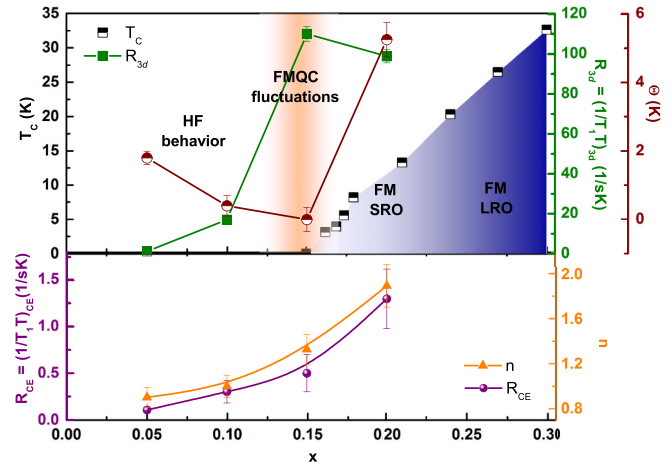


FIG. 6. Magnetic phase diagram ( $T_C$  data taken from Ref. [27]) and NQR parameters of our study as a function of Ge concentration. The half-filled circles correspond to the  $\Theta$  values.

crystalline sample with  $x = 0.05, 0.1$  (absent magnetic order),  $x = 0.15$  (nearly critical), and  $0.2$  ( $T_C \approx 6$  K). The nuclear quadrupolar resonance (NQR) spectra provide the evidence for the absence of strong intrinsic disorder due to Ge doping. Even more important, the spin-lattice relaxation rate provides the hyperfine field fluctuations on the Ga1 and Ga2 sites at zero field as an intrinsic measure of the Fe  $3d$  correlations. For the critical concentration of  $x = 0.15$ ,  $^{71}(1/T_1 T)$  diverges at  $T \rightarrow 0$  following a  $T^{-4/3}$  power law over two orders of magnitude in temperature, which indicates very pure 3D quantum critical FM fluctuations. For the  $x = 0.2$  sample, short-range order is found and  $^{71}(1/T_1 T)$  could be fitted well in the frame of Moriya's SCR theory for weakly FM systems. In contrast to that, low Ge substitutions in  $\text{FeGa}_3$  cause the formation of heavy fermions, as evidenced by the divergence of  $C(T)/T$  towards lowest temperatures. The coexistence of correlated  $3d$  electrons and the ferromagnetic short-range magnetic order in a very narrow stoichiometric range is found. We conclude that  $\text{FeGa}_{3-x}\text{Ge}_x$  is a platform to study the rare occurrence of  $3d$  heavy fermions in the vicinity of a quantum critical point with very pronounced 3D FM fluctuations, which is a rather unique scenario.

*Note added.* Recently, we became aware of a paper on Moessbauer measurements on  $\text{Fe}(\text{Ga},\text{Ge})_3$ . This local zero-field method strongly supports the results presented here [43]. In particular, the presence of antiferro- and ferromagnetic spin density and, most important, localized Fe moments is evidenced from their data.

### ACKNOWLEDGMENTS

We thank Professor H. Yasuoka for fruitful discussions on NQR and M. Brando for discussions on the FM critical point. Furthermore, discussions with H. Rosner and D. Kasinathan are acknowledged.



- [1] P. Gegenwart, Q. Si, and F. Steglich, *Nat. Phys.* **4**, 186 (2008).
- [2] Q. Si and F. Steglich, *Science* **329**, 1161 (2010).
- [3] J. Custers, K.-A. Lorenzer, M. Müller, A. Prokofiev, A. Sidorenko, H. Winkler, A. M. Strydom, Y. Shimura, T. Sakakibara, R. Yu, Q. Si, and S. Paschen, *Nat. Mater.* **11**, 189 (2012).
- [4] G. R. Stewart, *Rev. Mod. Phys.* **73**, 797 (2001).
- [5] M. Brando, D. Belitz, F. M. Grosche, and T. R. Kirkpatrick, [arXiv:1502.02898](https://arxiv.org/abs/1502.02898).
- [6] C. Pfleiderer, G. J. McMullan, S. R. Julian, and G. G. Lonzarich, *Phys. Rev. B* **55**, 8330 (1997).
- [7] T. Westerkamp, M. Deppe, R. KÜchler, M. Brando, C. Geibel, P. Gegenwart, A. P. Pikul, and F. Steglich, *Phys. Rev. Lett.* **102**, 206404 (2009).
- [8] T. Vojta, *J. Low Temp. Phys.* **161**, 299 (2010).
- [9] R. Hu, Kefeng Wang, Hyejin Ryu, Hechang Lei, E. S. Choi, M. Uhlarz, J. Wosnitza, and C. Petrovic, *Phys. Rev. Lett.* **109**, 256401 (2012).
- [10] C. J. Pedder, F. Kruger, and A. G. Green, *Phys. Rev. B* **88**, 165109 (2013).
- [11] J. L. Sarrao, R. Modler, R. Movshovich, A. H. Lacerda, D. Hristova, A. L. Cornelius, M. F. Hundley, J. D. Thompson, C. L. Benton, C. D. Immer, M. E. Torelli, G. B. Martins, Z. Fisk, and S. B. Oseroff, *Phys. Rev. B* **57**, 7785 (1998).
- [12] A. Fernandez-Pañella, D. Braithwaite, B. Salce, G. Lapertot, and J. Flouquet, *Phys. Rev. B* **84**, 134416 (2011).
- [13] K. Ishida, K. Okamoto, Y. Kawasaki, Y. Kitaoka, O. Trovarelli, C. Geibel, and F. Steglich, *Phys. Rev. Lett.* **89**, 107202 (2002).
- [14] P. Gegenwart, T. Westerkamp, C. Krellner, Y. Tokiwa, S. Paschen, C. Geibel, F. Steglich, E. Abrahams, and Q. Si, *Science* **315**, 969 (2007).
- [15] A. Steppke, R. KÜchler, S. Lausberg, E. Lengyel, L. Steinke, R. Borth, T. Luhmann, C. Krellner, M. Nicklas, C. Geibel, F. Steglich, and M. Brando, *Science* **339**, 933 (2013).
- [16] T. R. Kirkpatrick and D. Belitz, *Phys. Rev. B* **85**, 134451 (2012).
- [17] A. V. Chubukov, C. Pepin, and J. Rech, *Phys. Rev. Lett.* **92**, 147003 (2004).
- [18] G. J. Conduit, A. G. Green, and B. D. Simons, *Phys. Rev. Lett.* **103**, 207201 (2009).
- [19] D. Moroni-Klementowicz, M. Brando, C. Albrecht, W. J. Duncan, F. M. Grosche, D. Gruner, and G. Kreiner, *Phys. Rev. B* **79**, 224410 (2009).
- [20] Y. Horie, S. Kawashima, Y. Yamada, G. Obara, and T. Nakamura, *J. Phys.: Conf. Ser.* **200**, 032078 (2010).
- [21] P. Khuntia, A. M. Strydom, L. S. Wu, M. C. Aronson, F. Steglich, and M. Baenitz, *Phys. Rev. B* **86**, 220401(R) (2012).
- [22] P. Khuntia, P. Peratheepan, A. M. Strydom, Y. Utsumi, K.-T. Ko, K.-D. Tsuei, L. H. Tjeng, F. Steglich, and M. Baenitz, *Phys. Rev. Lett.* **113**, 216403 (2014).
- [23] S. Paschen, *Thermoelectrics Handbook, Macro to Nano*, edited by D. M. Rowe (CRC Press, Boca Raton, FL, 2005).
- [24] M. Wagner-Reetz, D. Kasinathan, W. Schnelle, R. Cardoso-Gil, H. Rosner, Y. Grin, and P. Gille, *Phys. Rev. B* **90**, 195206 (2014).
- [25] M. Wagner-Reetz, R. Cardoso-Gil, and Y. Grin, *J. Electron. Mater.* **43**, 1857 (2014).
- [26] K. Urmeo, Y. Hadano, S. Narazu, T. Onimaru, M. A. Avila, and T. Takabatake, *Phys. Rev. B* **86**, 144421 (2012).
- [27] N. Haldolaarachchige, J. Prestigiacomo, W. Adam Phelan, Y. M. Xiong, Greg McCandless, Julia Y. Chan, J. F. DiTusa, I. Vekhter, S. Stadler, D. E. Sheehy, P. W. Adams, and D. P. Young, [arXiv:1304.1897](https://arxiv.org/abs/1304.1897).
- [28] A. A. Gippius, M. Baenitz, K. S. Okhotnikov, S. Johnsen, B. Iversen, and A. V. Shevelkov, *Appl. Magn. Reson.* **45**, 1237 (2014).
- [29] A. A. Gippius, V. Yu. Verchenko, A. V. Tkachev, N. E. Gervits, C. S. Lue, A. A. Tsirlin, N. Büttgen, W. Krätschmer, M. Baenitz, M. Shatruk, and A. V. Shevelkov, *Phys. Rev. B* **89**, 104426 (2014).
- [30] D. J. Singh, *Phys. Rev. B* **88**, 064422 (2013).
- [31] V. Yu. Verchenko, M. S. Likhano, M. A. Kirsanova, A. A. Gippius, A. V. Tkachev, N. E. Gervits, A. V. Galeeva, N. Büttgen, W. Krätschmer, C. S. Lue, K. S. Okhotnikov, and A. V. Shevelkov, *J. Solid State Chem.* **194**, 361 (2012).
- [32] See Supplemental Material at <http://link.aps.org/supplemental/10.1103/PhysRevB.93.064410> for sample synthesis, chemical characterizations, magnetization, and specific-heat measurements and NQR measurements.
- [33] A. Ishigaki and T. Moriya, *J. Phys. Soc. Jpn.* **65**, 3402 (1996).
- [34] T. Moriya, *Spin Fluctuations in Itinerant Electron Magnetism* (Springer-Verlag, New York, 1985).
- [35] M. Majumder, K. Ghoshray, A. Ghoshray, B. Bandyopadhyay, B. Pahari, and S. Banerjee, *Phys. Rev. B* **80**, 212402 (2009).
- [36] M. Majumder, K. Ghoshray, A. Ghoshray, B. Bandyopadhyay, and M. Ghosh, *Phys. Rev. B* **82**, 054422 (2010).
- [37] Z. Nussinov, I. Vekhter, and A. V. Balatsky, *Phys. Rev. B* **79**, 165122 (2009).
- [38] H. Nakamura, M. Shiga, Y. Kitaoka, K. Asayama, and K. Yoshimura, *J. Phys. Soc. Jpn. Suppl. B* **65**, 165 (1996).
- [39] N. Büttgen, R. Böhmer, A. Krimmel, and A. Loidl, *Phys. Rev. B* **53**, 5557 (1996).
- [40] Y. Kuramoto and Y. Kitaoka, *Dynamics of Heavy Electrons* (Oxford Science, New York, 2000).
- [41] D. E. MacLaughlin, *Hyperfine Interact.* **49**, 43 (1989).
- [42] D. L. Cox, N. E. Bickers, and J. W. Wilkins, *J. Appl. Phys.* **57**, 3166 (1985).
- [43] J. C. Alvarez-Quiceno, M. Cabrera-Baez, J. Munevar, H. Micklitz, E. M. Bittar, E. Baggio-Saitovitch, R. A. Ribeiro, G. M. Dalpian, J. M. Osorio-Guillen, and M. A. Avila, [arXiv:1506.07159](https://arxiv.org/abs/1506.07159).